International Journal of Agriculture, Environment and Bioresearch

Vol. 2, No. 04; 2017

ISSN: 2456-8643

A 3-PARAMETER EMPIRICAL MODEL TO PREDICT EXTREME RAINFALL RATES IN THE NORTH-EAST OF ALGERIA.

Salima Guechi, Laroussi Beloulou, Saadane Djorfi, Hadjer Benzine, Halima Maalem, Wassila Saaidia
Laboratoire Ressources Naturelles et Aménagement, Université Badji Mokhtar, Annaba 23000, Algérie

ABSTRACT

This paper explores the data from more than twenty rainfall recording gages to develop Intensity Duration Frequency (IDF) relationships in the north-eastern part of Algeria. Using non parametric tests, a primary screening of rainfall data has been carried out to check that the annual time series variates are random, homogeneous and doen not contain any outlier. Severe storm intensities are calculated for various recurrence intervals using the General Extreme Value (GEV) probability distribution law. A three parameter geometric model that relates intensity to duration and return period, with highly significant correlation, is developed for each rainfall station. Such models, that describe the rainfall characteristics are useful tools in water structures design and rainfall-runoff modelling. They readily give the expected rainfall intensity of a given duration of storm having desired frequency of occurrence.

Keywords: North-east of Algeria, severe storm, GEV distribution, IDF model parameters.

1. Introduction

Urban and rural storm water management and engineering infrastructures designed to withstand floods generated by severe storm events are practically based on the concept of rainfall Intensity-Duration-Frequency (IDF) curves. Worldwide studies on the rainfall IDF relationships have received much attention in past decades and continue to challenge hydrologists as they are affected by climate change [1]- [11]. Furthermore, IDF curves are still in use today by water resources engineers as they can be readily applied to estimate the design runoff in water related projects. This work presents a straightforward method to develop IDF models using extreme rainfall rate data of twenty four available rainfall recording gauges that spread over the north-eastern part of Algeria for different observation periods. Such curves are commonly developed using historical annual maximum precipitation data fitted to a probability distribution to estimate the rainfall intensity (I) for given storm duration (D) and return period (T). So, the construction of these curves follows some steps where frequency analysis and regression are the basic methods used to establish such relationships in graphical or mathematical forms.

2. Material and Methods

Study area

Vol. 2, No. 04; 2017

ISSN: 2456-8643

Located in north-eastern Algeria, the study area extends over a length of about 300 km from Jijel in the West to the Tunisian border in the East and over a width of 250 km from North to South. It is located, to a large extent, north of the Tellian Atlas. It is roughly limited between the 35° and 37° North parallels and the 5° and 8°30' East meridians (Figure 1). This zone is limited to the North by the Mediterranean Sea, to the South and Southeast by Chott Melhrir and the Hauts Plateaux Constantine's basins, to the East by the Algerian-Tunisian border and finally by the Soummam watershed to the West. It encompasses thoroughly or partly, five major hydrographic basins: Côtiers Constantinois (03), Hauts Plateaux Constantinois (07), Kébir - Rhumel (10), Medjerda-Mellegue (12) and Seybouse (14) and spans over twelve wilayates (states) namely, Jijel, Mila, Constantine, Skikda, Annaba, Guelma, El Tarf, Tebessa, Souk Ahras, Oum El Bouaghi, Batna and Khenchela.

The northeastern Algeria is subject to the Mediterranean type climate characterized by a dry and warm period (May -October) and a wet and relatively cold season (November-April). The rainfall pattern is governed by the three classical rainfall laws; distance from the sea, elevation and exposure to northwesterly humid winds and currents. The Atlas Mountains play a major role as they constitutes a natural barrier to atmospheric disturbances from the North and West and subdivides the region into two separate slopes; the very humid North Slope with abundant vegetation cover (Edough and Collo massifs forests) and the relatively drier or even semi-arid South slope where the vegetation cover becomes less dense and sparse (Constantine High Plains and Steppe Zone).

The yearly rainfall gradient is slightly increasing from East to West (700-1500 mm) and remarkably decreasing from North to South (less than 300 mm in Tebessa City).

In recent years, this part of the country has experienced several floods due to severe storm events that caused property damages and human losses [12]-[15].

Vol. 2, No. 04; 2017

ISSN: 2456-8643

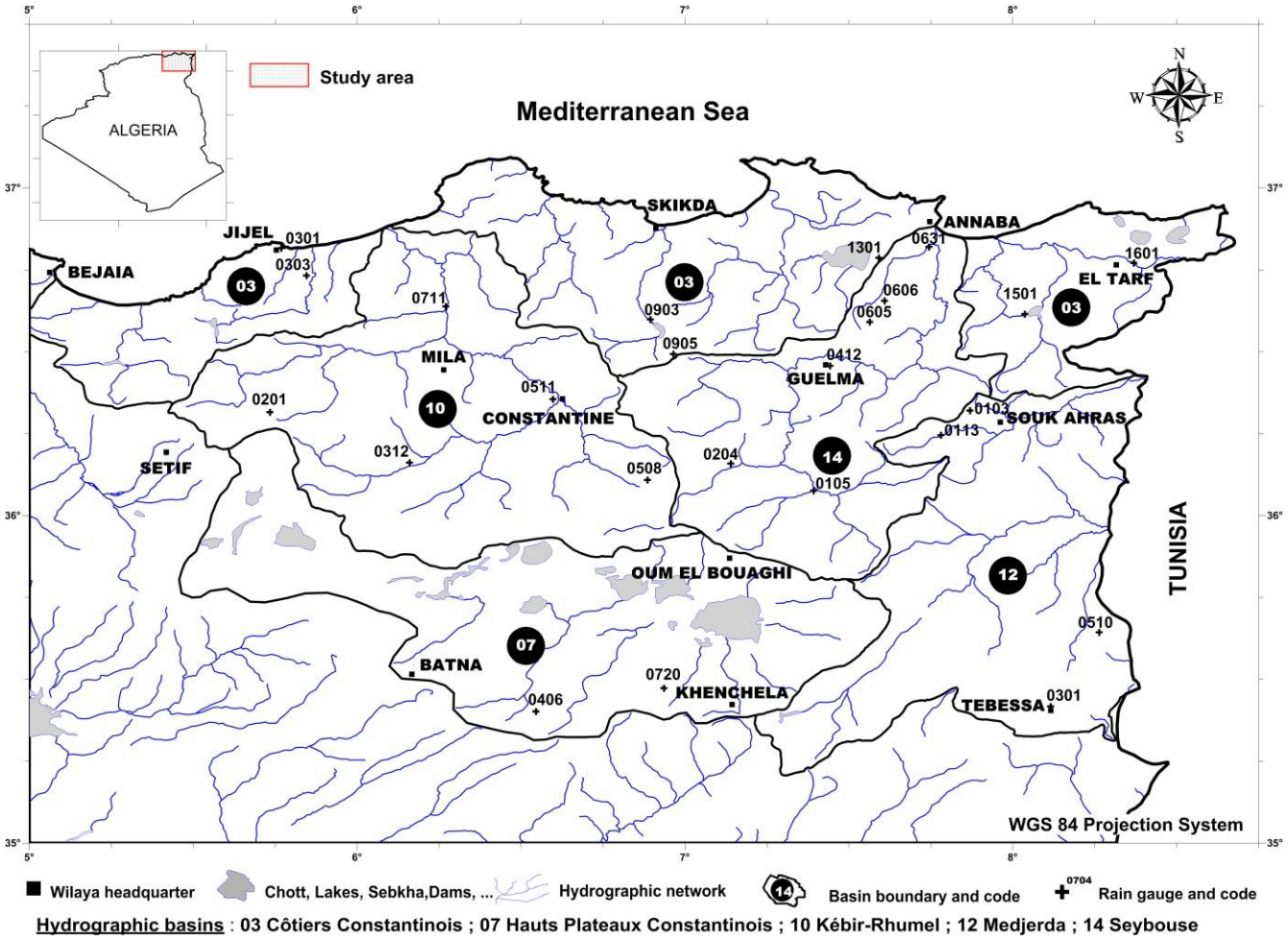

Sampling techniques and data processing

From rainfall charts, provided by the National Agency for Water Resources (ANRH), the entire rainfall records in a year is analyzed to select relevant rainfall events in order to find the maximum depths and intensities for various storms of constant duration (D). The procedure involves calculating automatically moving sums at a one-minute me step over the duration of the storm using linear interpolation integrated in the application 'Averse 2.0'.

The maximum rainfall depth (H) and rate (I), the ratio of depth to duration, values over specified durations ranging from 5 minutes to 24 hours are displayed. The largest of all such values is taken to be the maximum depth (intensity) in that year for that duration. Rainfall intensity data

Vol. 2, No. 04; 2017

ISSN: 2456-8643

are then organized into an annual maximum series. Seventeen time series that behave as random variables of different sample sizes are obtained for 24 rain gauges in the study area (Table 1). A raw database for short duration rainfall intensity is hence constructed.

Table 1: Identification of rainfall stations

Rain gauge name	*Code*	*Latitude*	*Longitude*	*Elevation (m)*	*Observation period*	*Number of years*	*Processed storm events*
Côtiers Constantinois basin (03)							
Jijel	*0301*	*36.82°N*	*5.77°E*	*5*	*1984/2002*	*18*	*303*
El Agrem	*0303*	*36.44°N*	*5.50°E*	*-*	*2001/2006*	*5*	*90*
Zardezas Dam	*0903*	*36.60°N*	*6.89°E*	*200*	*1984/1996*	*9*	*130*
Bousnib	*0905*	*36.50°N*	*6.96°E*	*900*	*1960/2002*	*24*	*1216*
Fetzara Lake	*1301*	*36.79°E*	*7.59°E*	*15*	*1973/1981*	*8*	*69*
Chaffia Dam	*1501*	*36.61°N*	*8.04°E*	*170*	*1987/1996*	*10*	*181*
Ain Assel	*1601*	*36.77°N*	*8.36°E*	*32*	*1970/2005*	*32*	*550*
Hauts Plateaux Constantinois basin (07)							
Foum Toub	*0406*	*35.41°N*	*6.55°E*	*1102*	*1969/2004*	*29*	*219*
Foum el Gueis	*0720*	*35.50°N*	*6.94°E*	*945*	*1987/1997*	*10*	*96*
Kébir-Rhumel basin (10)							
Redjas Ferada	*0201*	*36.42°N*	*6.12°E*	*360*	*1973/1979*	*7*	*45*
Chelgoum Laid	*0312*	*36.16°N*	*6.16°E*	*768*	*1984/1992*	*9*	*378*
Ouled Rahmoun	*0508*	*36.18°N*	*6.70°E*	*700*	*1984/1993*	*9*	*85*
El Fourchi	*0511*	*36.36°N*	*6.59°E*	*775*	*1974/1982*	*7*	*35*
Settara	*0711*	*36.72°N*	*6.34°E*	*280*	*1972/2002*	*31*	*286*
Medjerda-Mellegue basin (12)							
Ain Seynour	*0103*	*36.32°N*	*7.87°E*	*904*	*1996/2000*	*5*	*54*
Cheikh Abdallah[1]	*0113*	*36.25°N*	*7.78°E*	*700*	*-*	*100*	*40*
Tébessa	*0301*	*35.40°N*	*8.12°E*	*890*	*1974/2005*	*31*	*> 361*
Ain Zerga[2]	*0510*	*35.64°N*	*8.26°E*	*850*	*-*	*100*	*98*
Seybouse basin (14)							
Aioun Settara	*0105*	*36.07°N*	*7.39°E*	*741*	*1972/2004*	*27*	*148*
Tamlouka	*0204*	*36.16°N*	*7.14°E*	*740*	*1971/1979*	*8*	*46*
Guelma Lycée	*0412*	*36.46°N*	*7.44°E*	*260*	*1974/2001*	*27*	*273*
Nechmaya	*0605*	*36.59°N*	*7.56°E*	*265*	*1975/1979*	*3*	*4*
Ain Berda	*0606*	*36.66°N*	*7.61°E*	*100*	*1978/1999*	*22*	*322*
Pont Bouchet	*0631*	*36.82°N*	*7.74°E*	*3*	*1976/2005*	*29*	*364*

[1, 2] stochastically *generated random variables from Depth-Duration-Frequency curves calculated by the ANRH.*

Vol. 2, No. 04; 2017

ISSN: 2456-8643

3. Frequency analysis and probabilistic model selection

An IDF curve gives the expected rainfall intensity of a given duration of storm having desired frequency of occurrence. It may be represented in graphical or mathematical forms. Once a reliable database is constructed, the method used to estimate the relationships describing the IDF curves is classical. It follows three distinct steps and has already been used by many authors [16]-[20]: probability distribution fitting to the annual series for each duration of aggregation, storm intensity estimation for each duration and specified return periods, based on the densities estimated in the first step and curvilinear regression between rainfall rate (as explained variable) estimated in the second step and storm duration (as input variable). The least squares method allows estimating the parameters of the empirical IDF relationships. The procedure is outlined in the chart below (Fig. 2).

For each rainfall recorder, the seventeen time series (raw data) are subjected to an exploratory analysis to check the reliability of data for frequency analysis using graphical and non parametric tests for randomness, homogeneity and outliers detection. As a result, eighteen rain gauges containing at least seven complete years of observations are retained for constructing IDF curves that may be considered useful in practice. The remaining ones are discarded for insufficient sample size for reliable frequency analysis (El Agrem, Ain Seynour and Nechmaya) or identified as containing anomalous and questionable data sets (Zardezas Dam, Fetzara Lake and El Fourchi) when compared to nearby rain gauges.

The goodness of fit is appreciated by a combination of graphical and numerical techniques including the quantile-quantile and probability-probability plots, the Kolmogorov-Smirnov (D), Anderson-Darling, (W^2) and Pearson (χ^2) tests integrated in the Mathwave Technologies Company Easyfit software. Since graphical techniques provide a visual comparison of simulated and measured data and a first overview of model performance, the assessment of the probability distribution models is basically appreciated by the total test score obtained from all the three numerical tests. Test scores ranging from one to six (1-6) are awarded to each distribution model based on the criteria that the distribution with the lowest total score is chosen as the best distribution model for the data of a particular rain gauge. In general, the distribution best supported by a test is attributed a score of one (1), the next best is awarded two (2), and so on in ascending order. A distribution is not taken into account if the test indicates that there is a significant difference between the predicted and observed rainfall values.

Vol. 2, No. 04; 2017

ISSN: 2456-8643

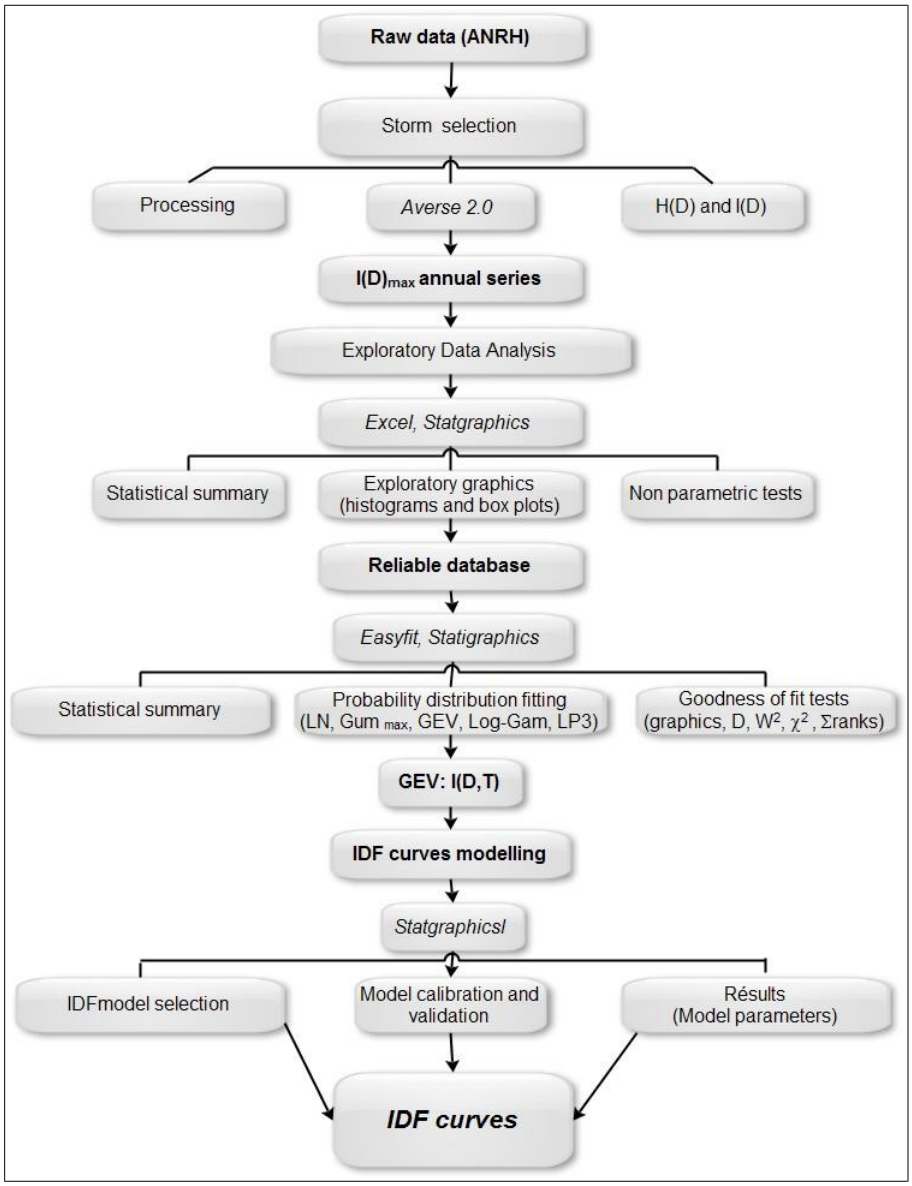

Figure2: Detailed procedure to calculate IDF curves

For every test category, overall ranks of each distribution are obtained by summing the individual point rank at each rain gauge. Since the rainfall time series are relatively short [27] and the overall rank sum is minimum, the General Extreme Value distribution is preferred, over the log-Pearson III model, to calculate rainfall intensities for 16 specified recurrence intervals (T) between 2 and 100 years for each of the durations being considered (Table 2).

Vol. 2, No. 04; 2017

ISSN: 2456-8643

Table 2: Probabilistic model selection by the overall minimum rank sum method

Rain gauge	Probability distribution model					
	LN-2p	LN-3p	Gumbel max	GEV	LG-2p	LP3
Jijel	249	167	228	116	172	137
Bousnib	99	68	88	37	120	74
Chaffia	169	110	179	126	176	104
Ain Assel	216	121	249	114	225	146
Foum Toub	234	171	196	108	217	131
Foum Gueis	164	147	155	78	95	80
Redjas Ferada	167	135	156	75	115	67
Chelgoum	71	48	81	37	56	43
Ouled Rahmoun	165	149	152	47	130	78
Settara	76	70	97	51	94	92
Cheikh Abdallah	73	45	54	37	35	32
Tebessa	232	117	250	129	185	147
Ain Zerga	52	83	79	30	63	53
Aioun Settara	193	151	257	103	163	132
Tamlouka	151	151	135	84	122	71
Guelma	215	160	236	105	177	139
Ain Berda	223	190	218	92	183	147
Pont Bouchet	204	172	254	107	173	155
Overall rank sum	2953	2255	3064	**1476**	2501	1828

Hence, the T-year maximum rainfall intensity is estimated for each duration using the General Extreme Value distribution with k, σ and μ as the shape, scale and location parameters, respectively. For example, Table 3 presents the predicted T-year maximum intensity for rainfall recorded at the Foum el Gueis rain gauge.

Table 3: Rainfall Intensity-Duration-Frequency at the Foum el Gueis rain gauge

GEV distribution parameters	Rainfall duration										
	Minutes				Hours						
	5	15	30	…	1	2	3	6	…	12	24
k	-0.122	-0.009	0.078	…	-0.073	-0.216	-0.195	0.043	…	-0.068	0.12
σ	33.306	10.742	5.998	…	3.138	0.882	0.663	0.681	…	0.5449	0.427
μ	91.302	41.052	20.762	…	12.713	6.892	5.269	3.633	…	2.254	1.347
T (years)	T-year rainfall intensity (mm/h)										
2	103.2	45.0	23.0	…	13.9	7.2	5.5	3.9	…	2.5	1.5
5	137.0	57.1	30.3	…	17.2	8.0	6.1	4.7	…	3.0	2.1
10	156.8	65.0	35.5	…	19.2	8.5	6.5	5.2	…	3.4	2.5
15	167.2	69.4	38.6	…	20.3	8.7	6.7	5.6	…	3.6	2.7
20	174.3	72.5	40.8	…	21.1	8.8	6.8	5.8	…	3.7	2.9
25	179.5	74.9	42.6	…	21.7	8.9	6.9	6	…	3.8	3.0
30	183.9	77.0	44.1	…	22.1	9.0	6.9	6.1	…	3.9	3.1
35	186.7	78.3	45.1	…	22.5	9.1	7.0	6.2	…	4.0	3.2
40	189.9	79.9	46.3	…	22.8	9.1	7.0	6.3	…	4.0	3.3
45	192.7	81.2	47.3	…	23.1	9.2	7.1	6.5	…	4.1	3.4
50	194.7	82.2	48.1	…	23.4	9.2	7.1	6.5	…	4.1	3.5
60	198.0	83.9	48.5	…	23.8	9.3	7.1	6.7	…	4.2	3.6
70	202.0	85.9	51.1	…	24.2	9.4	7.2	6.8	…	4.3	3.7
80	205.0	87.5	52.4	…	24.6	9.4	7.2	6.9	…	4.3	3.8
90	206.7	88.4	53.1	…	24.8	9.4	7.3	7.0	…	4.4	3.9
100	208.5	89.4	54.0	…	25.0	9.5	7.3	7.1	…	4.4	4.0

4. IDF curves relationship-Derivation of IDF equations

In order to represent frequency analysis results in a much more explicit manner, the rainfall IDF curves were calculated for 18 rainfall sites. A mathematical model synthesizing the Intensity-Duration-Frequency relationship is therefore preferred. Scatter diagrams show that the longer the duration, the lower average rainfall intensity for a given return period. It is also true that the longer the recurrence interval, the greater the precipitation intensity for a given storm duration. The relation between these three components, storm duration (D), storm intensity (I) and storm

Vol. 2, No. 04; 2017

ISSN: 2456-8643

return period (T), is represented by a family of curves called the intensity- duration-frequency curves, or IDF curves that are not presented here for space limitations. They can be modeled by mathematical formulas such as:

Wenzel [2]: $I = \frac{a}{D^b + f}$ (1)

Horner [28]: $I = \frac{a}{(D+f)^b}$ (2)

Bernard [29]: $I = \frac{cT^m}{D^b}$ (3)

Sherman [30]: $I = \frac{cT^m}{(D+f)^b}$ (4)

where I is the rainfall intensity (mm/h), D is the duration (minutes), T is the recurrence period (years), a, b, c, f and m are regional model calibration constants to be obtained with regression analysis techniques. Since the expression in the nominator of equations (1) through (4) is independent of the aggregation time and completely determined by the probability distribution function of the annual maximum rainfall intensity [17], the Bernard type model is adopted in this work; the others are discarded to avoid over-parameterization. Note that letting $f = 0$ and $a = cT^m$, the above equations are the same.

To determine the model parameters, the first step is to fit an increasing power model that relates probable maximum intensity I(T), as target variable, to duration D, the input variable, using least squares techniques implemented in the Statgraphics Centurion XV software. The basic results for the Foum el Gueis rain gauge are presented in Table 4.

Table4 : Foum el Gueis station (070720) - Linear regression outputs

T (yr)	2	5	10	15	20	25	30	35	40	45	50	60	70	80	90	100
a	302.3	375.3	418.2	440.7	456.3	467.2	476.3	480.8	487.2	490.9	495.4	499.7	509.8	515.7	516.7	521.0
b	0.74	0.74	0.74	0.74	0.74	0.74	0.74	0.73	0.73	0.73	0.73	0.73	0.73	0.73	0.72	0.72
r^2	0.99	0.99	0.98	0.98	0.97	0.97	0.97	0.99	0.97	0.97	0.96	0.96	0.96	0.96	0.96	0.96

The relationship I(D, T) is found to be highly significant for all sites (the coefficient of determination R^2 is greater than 90% for all cases). The parameter a increases as the recurrence period (T) does while the parameter b varies slightly and the average value $\bar{b}$ is retained for the model calibration. In the second step, an in-depth analysis of the relationship between the parameter a and frequency (T) is needed to fully define the model. Dispersion diagrams of the

a(T) function suggest, once more, that an increasing geometric relationship can be fitted. This relation takes the form:

$$a = cT^m \quad (5)$$

where the constants c and m and the goodness of fit are similarly estimated by regression analysis. Finally, the 3-parameter Bernard type model that incorporates the recurrence interval is completely defined for eighteen gauging stations in the study area (Table 5). For example, the IDF model for the Foum el Gueis station is:

$$I = \frac{301T^{0.127}}{D^{0.73}} \quad (6)$$

5. Model validation

The fact that the performances of the model calibration are less indicative of its actual simulation capabilities, these are best expressed through validation, an absolutely primordial step in the modeling process of random events.

A model is considered as valid if it reproduces correctly the data. There is no universal technique to evaluate the performance of a model. The basic principle is to compare predicted (or simulated) variates with sampled data. To appreciate the efficiency of the model, calculations are generally performed on data that were not used in its calibration.

Table 5: IDF Model calibration and validation parameters for various rainfall stations in the Northestern Algeria

Rain gauge name	*Model calibration parameters*				*Model performance criteria*				
	c	*m*	*b*	R^2	R^2	*NSE*	d_0	d_1	d_2
Côtiers Constantinois basin (03)									
Jijel	*199.87*	*0.377*	*0.70*	*0.99*	*0.83*	*0.67*	*0.94*	*0.86*	*0.86*
Bousnib	*192.2*	*0.126*	*0.60*	*0.63*	*0.99*	*0.98*	*0.99*	*0.96*	*0.96*
Chaffia Dam	*221.9*	*0.27*	*0.65*	*0.98*	*0.99*	*0.98*	*0.99*	*0.94*	*0.94*
Ain Assel	*130.52*	*0.450*	*0.67*	*0.99*	*0.99*	*0.98*	*0.99*	*0.94*	*0.94*

Table 5: continued

Rain gauge name	*Model calibration parameters*				*Model performance criteria*				
	c	*m*	*b*	R^2	R^2	*NSE*	d_0	d_1	d_2
Hauts Plateaux Constantinois basin (07)									
Foum Toub	*206.5*	*0.382*	*0.74*	*0.96*	*0.98*	*0.97*	*0.99*	*0.93*	*0.99*
Foum el Gueis	*301.0*	*0.127*	*0.73*	*0.95*	*0.98*	*0.94*	*0.98*	*0.91*	*0.92*
Kébir-Rhumel basin (10)									
Redjas Ferada	*165.7*	*0.314*	*0.69*	*0.98*	*0.97*	*0.97*	*0.99*	*0.92*	*0.92*
Chelgoum Laid	*252.7*	*0.158*	*0.69*	*0.94*	*0.99*	*0.99*	*0.99*	*0.98*	*0.98*
Ouled Rahmoun	*159.46*	*0.315*	*0.67*	*0.99*	*0.98*	*0.94*	*0.98*	*0.92*	*0.92*
Settara	*73,2*	*0,382*	*0.56*	*0.98*	*0.97*	*0.85*	*0.97*	*0.89*	*0.88*
Medjerda-Mellegue basin (12)									
Cheikh Abdallah	*134.33*	*0.38*	*0.66*	*0.98*	*0.69*	-	*0.61*	*0.68*	*0.73*
Tébessa	*215.68*	*0.331*	*0.74*	*0.95*	*0.99*	*0.98*	*0.99*	*0.94*	*0.94*
Ain Zerga	*314.00*	*0.16*	*0.73*	*0,94*	*0.94*	*0.97*	*0.99*	*0.95*	*0.95*
Seybouse basin (14)									
Aioun Settara	*109.6*	*0.528*	*0.73*	*0.99*	*0.86*	-	*0.88*	*0.81*	*0.78*
Tamlouka	*280.32*	*0.362*	*0.82*	*0.96*	*0.99*	*0.98*	*0.99*	*0.94*	*0.94*
Guelma Lycée	*196.29*	*0.287*	*0.69*	*0.94*	*0.99*	*0.98*	*0.99*	*0.93*	*0.93*
Ain Berda	*164.2*	*0.208*	*0.60*	*0.99*	*0.96*	*0.92*	*0.98*	*0.91*	*0.91*
Pont Bouchet	*187.52*	*0.142*	*0.57*	*0.99*	*0.95*	*0.90*	*0.98*	*0.94*	*0.94*

Vol. 2, No. 04; 2017

ISSN: 2456-8643

In applied hydrology, many criteria are used to assess the model sensitivity, including the correlation coefficient or its squared value (the coefficient of determination), the mean squared error, the Nash criterion of efficiency, the Willmott indices of agreement and the Kling–Gupta efficiency (KGE) index [31], [32], [33], [34] and [35].

In this paper, the following "goodness-of-fit" measures are used for model validation: the coefficient of correlation (R), the Nash-Sutcliffe criterion of efficiency (NSE) and the Willmott indices of agreements d_i) which are briefly described here. The Pearson's product-moment or correlation coefficient, a measure of the strength and direction of the linear relationship between two variables with N paired observations, is given by:

$$R = \left[\frac{\sum_1^N (O_i - \bar{O}) \times (P_i - \bar{P})}{\sqrt{\{\sum_1^N (O_i - \bar{O})^2\}} \times \sqrt{\{\sum_1^N (P_i - \bar{P})^2\}}}\right] \quad (7)$$

where O_i and P_i are the explicative and explained variables with means $\bar{O}$ and $\bar{P}$, respectively. It (R) indicates how closely data in a scatter plot fall along a straight line. The closer that the absolute value of R is to one, the closer that the data are described by a linear equation.

The coefficient of efficiency has been widely used to evaluate the performance of hydrologic models. Nash and Sutcliffe defined this coefficient, which ranges from $-\infty$ to 1.0, with higher values (NSE $\geq$ 0.6) indicating better agreement, as:

$$NSE = 1 - \frac{\sum_1^N (O_i - P_i)^2}{\sum_1^N (O_i - \bar{O})^2} = 1 - \frac{MSE}{\sigma^2} \quad (8)$$

in which σ^2 is the observed data variance and the other terms are defined above. Physically NSE, is the ratio of the mean square error,

$$MSE = N^{-1} \times \sum_1^N (O_i - P_i)^2 \quad (9)$$

to the variance in the observed data σ^2, subtracted from unity.

The Willmott indices of agreement (d), are widely used dimensionless indicators of model performance. These are given by the following expressions:

$$d_0 = 1 - \frac{\sum_{i=1}^N (P_i - O_i)^2}{\sum_{i=1}^N [|P_i - \bar{O}| + |O_i - \bar{O}|]^2} \quad (10)$$

$$d_1 = 1 - \frac{\sum_{i=1}^N |P_i - O_i|}{\sum_{i=1}^N (|P_i - \bar{O}| + |O_i - \bar{O}|)} \quad (11)$$

Vol. 2, No. 04; 2017

ISSN: 2456-8643

$d_2 = 1 - \frac{\sum_{i=1}^{N}|P_i - O_i|}{2\sum_{i=1}^{N}|O_i - \bar{O}|}$ if

$$\sum_1^N |P_i - O_i| \leq 2 \times \sum_1^N |O_i - \bar{O}| \qquad (12)$$

Each of these indices of agreement varies from -∞ to 1 with higher values indicating that the model predicted values have better agreement with the observations [32].

In this paper, predicted data with the Bernard 3-parameter model, for a return period close to twice the sample size (T ≈ 2N), are compared with the highest storm intensity data recorded over any specified duration during the whole observation period of N years at each calibration rainfall gauge. The model calibration and validation processes results are reported in Table (5)

Performances, expressed in terms of Pearson correlation, Nash-Sutcliffe criterion and Willmott indices of agreement obtained by applying the 3-parameter Bernard type model are satisfactory to good ($0.86 \leq R^2 \leq 0.99$; $0.67 \leq NSE \leq 0.99$; $0,78 \leq d_2 \leq 0,99$) in calibration and in validation phases. Furthermore, the correlation coefficient values being close to one for both calibration and validation cases indicate a strong relationship between observed and simulated values. In other words, the "goodness of fit" criteria imply that the 3-parameter model works sufficiently well and provides satisfactory answers as to simulate severe storms intensities in the North-east of Algeria.

6. Conclusion

This paper presents a 3-parameter multiplicative model to overcome the lack of information on short duration rainfall data at 18 sites with recording rainfall gauges in the north-eastern part of Algeria. The capability of the model to provide a reliable estimate of the short-duration design storm intensity is tested by computing the coefficient of determination which shows that more than 80 % of the variability is explained by the model for more than 95% of the recording gauges. Results of this evaluation indicate the feasibility of the proposed procedure for deriving the IDF curves relations for most rainfall stations with reliable data series in the study area. In its empirical form, the predictive model is used to estimate, with sufficient accuracy, the T-year design rainfall intensity for any duration. However, this set of mathematical equations that describe the IDF relationships and provide a practical solution to hydro technical projects in the Northeastern part of Algeria is not recommended to extrapolate IDF curves to T 's exceeding the precipitation record length more than twice. Finally, further work on areal mapping of the model parameters is also recommended as it might increase its applicability in this part of Algeria. Moreover, observed changes in rainfall characteristics due to climate changes suggest that IDF relationships be regularly updated to include more recent rainfall time series.

Vol. 2, No. 04; 2017

ISSN: 2456-8643

REFERENCES

[1] Bell, F. C. (1969). Generalized rainfall-duration frequency relationships, Journal of Hydraulics Engineering, ASAE, 95(1), 311-327.

[2] Wenzel H.G., (1982). Rainfall for urban storm water design. In Urban Storm Water Hydrology. Kibler, D.F. (editor). Water Resources Monograph, 7, AGU, Washington, DC.

[3] Guevara E., Márquez A. M., (2008). Regional Modeling of IDF Curves for Venezuela. 11th International Conference on Urban Drainage, Edinburgh, Scotland, UK.

[4] Simonovic S.P., Peck, A., (2009). Updated rainfall intensity duration frequency curves for the city of London under changing climate. Water Resources Research Report No: 065, UK.

[5] Elsebaie, I.H., (2012). Developing rainfall intensity-duration-frequency relationship for two regions in Saudi Arabia. J. King Saud Univ. Eng. Sci,, 24, 131–140.

[6] Rashid, M.M., Faruque, S.B., Alam, J.B., (2012). Modeling of short duration rainfall intensity duration frequency (SDR-IDF) equation for Sylhet City in Bangladesh. APRN Journ. Sci. Tech. 2 (2), 92–95.

[7] Bhatt, J.P., Gandhi, H.M., Gohil, K.B., (2014). Generation of intensity duration frequency curves using daily rainfall data for different return periods. J. Inter. Acad. Res. Multidiscip. 2 (2), 717–722.

[8] Yilmaz A, Perera B., (2014). Extreme rainfall nonstationarity investigation and intensity-frequency-duration relationship. Journ. Hydrol. Eng., 19, 1160–1172.

[9] Wayal, A.S., Menon, K., (2014). Intensity-duration-frequency curves and regionalization. Inter. J. Innovative Res. Adv. Eng., 1 (6), 28–32.

[10] De Paola F, Giugni M, Topa M.E, Bucchignani E., (2014). Intensity-Duration-Frequency (IDF) rainfall curves, for data series and climate projection in African cities. Springerplus, 9;3:133. doi: 10.1186/2193-1801-3-133. Retrieved from: https://www.ncbi.nlm.nih.gov/pmc/articles/PMC4320185/

[11] Bodian A., Dacosta A.H., Diouf R. N., Ndiaye E.H.O., Mendy A., (2016). Contribution à la connaissance de l'aléa pluvial au Sénégal grâce à la valorisation des données pluviographiques, Climatologie, Vol. 13, 38-46.

[12] Beloulou L., (2014). Vulnérabilité aux inondations en milieu urbain. Cas de la ville d'Annaba (Nord-Est algérien). Presses académiques francophones, OmniScriptum GmbH & Co. 420p.

[13] Lahlah S., (2004). Les inondations en Algérie. Actes des journées techniques : Risques naturels : inondation, prévision, protection, Batna 15 et 16 décembre, pp 43-59.

Vol. 2, No. 04; 2017

ISSN: 2456-8643

[14] Belagoune F., (2012): Etude et modélisation des crues des cours d'eau en milieu semi-aride. Cas des grands bassins versants 05, 06 et 07. Mémoire de magister, Département d'hydraulique et de génie civil, Université Kasdi merbah, Ouargla, 181p.

[15] Tahar S., (2013). Impact des inondations sur l'espace urbain. Le cas de la Wilaya de Sidi Bel Abbes. Mémoire de magister, Département de géographie et aménagement du territoire, université d'Oran, 160 p

[16] Demarée G., (1985). Intensity–duration–frequency relationship of point precipitation at Uccle. Reference period 1934–1983. Koninklijk Meteorologisch Instituut van België, Publications Reeks A, nr. 116.

[17] Koutsoyiannis, D., Kozonis, D. & Manetas, A., (1998). A mathematical framework for studying rainfall intensity-duration-frequency relationships. J. of Hydrol. 206, 118–135.

[18] Lam K.H., Milton J., Nadeau M., Vescovi L., (2004). Mise à jour des courbes d'Intensité Durée Fréquence des pluies de courte durée du climat récent au Québec. 57ème Congrès annuel de l'association canadienne des ressources hydriques-Eau et changement climatique: comprendre pour mieux s'adapter, 16-18 Juin, Montréal, Qc, Canada.

[19] Mohymont B., Démarée G.R., (2006). Courbes intensité-durée-fréquence des précipitations à Yangambi, Congo, au moyen de différents modèles de type Montana. Hydrological Sciences Journal, 51(2), 239-253.

[20] Kiingumbi A., Mailhot A., (2010). Courbes Intensité-Durée-Fréquence (IDF): comparaison des estimateurs des durées partielles et des maximums annuels. Hydrological Sciences Journal, 55(2), 162-176

[21] Tao, D.Q., Nguyen, V.T., Bourque, A., (2002). On selection of probability distributions for representing extreme precipitations in Southern Quebec. Annual Conference of the Canadian Society for Civil Engineering. 5th -8th June, 1-8.

[22] Topaloglu, F. (2002). Determining Suitable Probability Distribution Models for Flow and Precipitation Series of the Seyhan River Basin. Turk Journal of Agric.,26, 189 - 194.

[23] Zalina M.D., M. Desa M.N., Nguyen V.T.V., M. Kassim A.H., (2002). Selecting a probability distribution for extreme rainfall series in Malaysia. Water Science and Technology, 45(2), 63–68.

[24] Lee C., (2005). Application of rainfall frequency analysis on studying rainfall distribution characteristics of Chia-Nan plain area in Southern Taiwan. Journal of Crop, Environment & Bioinformatics, 2, 31-38.

[25] Olofintoye, O.O, Sule, B.F and Salami, A.W., (2009). Best-fit Probability distribution model for peak daily rainfall of selected Cities in Nigeria. New York Science Journal, 2(3), 1–12.

Vol. 2, No. 04; 2017

ISSN: 2456-8643

[26] Benabdesselam T., Amarchi H., (2013). Regional approach for the estimation of extreme daily precipitation on North-east area of Algeria. International Journal of Water Resources and Environmental Engineering, 5(10), 573-583.

[27] Svensson C., Jones D.A., (2010). Review of rainfall frequency estimation methods. Journal of Flood Risk Management, 3(4), 296–313.

[28] Horner, W., Flynt, F., (1936). Relation between rainfall and runoff from small urban areas. Trans. ASCE, 101, 104–183.

[29] Bernard M.M., (1932). Formulas for rainfall intensities of long durations. Trans. ASCE, 96, 592-624

[30] Sherman C.W., (1931). Frequency and Intensity of Excessive Rainfall at Boston, Mass. Trans. ASCE, 95, 951-960.

[31] B.P. Wilcox, W.J. Rawls, D.L. Brakensiek, J.R. Wight, Predicting runoff from rangeland catchments: A comparison of two models, Water Resour. Res., 26, 1990, pp. 2401-2410.

[32] D.R. Legates, G. J. McCabe Jr., Evaluating the use of "goodness-of-fit" Measures in hydrologic and hydroclimatic model validation, Water Resour. Res., 35(1), 1999, pp. 233–241.

[33] C. J. Willmott, S.M. Robesonb, Kenji Matsuura, A refined index of model performance, Int. J. Climatol., 32, 2012, pp. 2088–2094.

[34] Gupta H.V., Kling H., Yilmaz K. K, Martinez G. F., (2009). Decomposition of the mean squared error and NSE performance criteria: Implications for improving hydrological modelling. Journal of Hydrology, 377(1-2), 80-91.

[35] Nash J.E and J.V. Sutcliffe, 1970. River flow forecasting through conceptual models. Part I – A discussion of principles. Journal of Hydrology, Vol. 27, N°3: 282-290.